

Ancilla-assisted probing of temporal quantum correlations of large spins

Michael Kastner

*National Institute for Theoretical Physics (NITheP), Stellenbosch 7600, South Africa and
Institute of Theoretical Physics, Department of Physics, University of Stellenbosch, Stellenbosch 7600, South Africa
(Dated: December 22, 2024)*

When measuring quantum spins at two or more different times, the later measurements are affected by measurement backaction occurring due to the earlier measurements. This makes the measurement of temporal quantum correlation functions challenging. In Phys. Rev. A **96**, 022127 it has been shown that the disturbing effect of measurement backaction can be mitigated by using weak measurements instead of projective measurements. Such weak measurements are implemented by weakly coupling the system to ancilla degrees of freedom. The weaker the measurement strength, the better works the suppression of backaction effects, but the larger a measurement sample is needed. Here we show that, by using a spin-1/2 ancilla for probing a system consisting of spins with large spin quantum numbers $l \gg 1/2$, the weak-coupling requirement, and hence also the need for large measurement samples, can be dropped. A potential application of such a strong-coupling measurement protocol is the probing of an array of Bose–Einstein condensates by light.

I. INTRODUCTION

Temporal quantum correlations, like the two-point function $\langle O_1(t_1)O_2(t_2) \rangle$, allow for a detailed characterization of the nonequilibrium behavior of quantum systems, more detailed than what equal-time correlations can achieve. They feature in a broad variety of physical theories and applications, including fluctuation–dissipation relations and the Kubo formula [1], scattering theory and optical coherences [2], transport theory [3], and glassy dynamics and aging [4].

Experimentally such temporal correlation functions are not easily accessible, because naively measuring the observable O_1 at the early time t_1 induces a wave function collapse and hence affects the outcome of the measurement of the observable O_2 at the later time t_2 . To mitigate, or even avoid, measurement backaction, measurement protocols of varying generality and complexity have been proposed [5–9]. In the measurement scheme of Ref. [7], the disturbance due to measurement backaction is mitigated by using weak measurements where, instead of projectively measuring O_1 at the time t_1 , an ancilla degree of freedom is weakly coupled to O_1 in a suitable way. Subsequent measurement of the ancilla allows the experimenter to retrieve a small amount of information about the observable, while the state of the system, and hence also the outcome of a measurement of O_2 at time t_2 , is affected only mildly. Accumulating statistics over multiple repetitions of this weak measurement protocol then facilitates the reconstruction of the temporal two-point correlation function $\langle O_1(t_1)O_2(t_2) \rangle$ with only a small statistical error (controlled by the number of repetitions) and a small systematic error (determined by the weak coupling strength).

In this paper we show that, under some additional conditions, the weak-coupling requirement of such an ancilla-based measurement scheme is dispensable when the local Hilbert space dimension of the constituents of the system of interest is much larger than the Hilbert space dimension of the ancilla degree of freedom that is used for probing. The intuition behind this proposal is that, under these conditions, even for strong system–ancilla coupling, selection rules impose constraints on the effect of backaction. As an example, the reader may think of a chain of spin- l degrees of freedom, probed by coupling

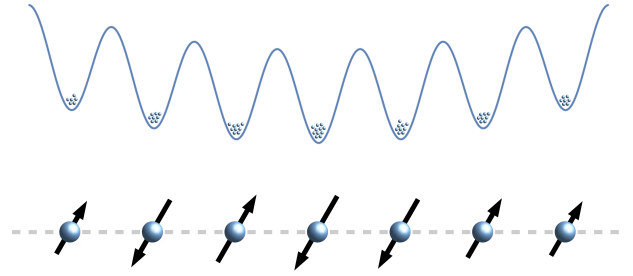


FIG. 1. Top: A sinusoidal optical lattice, superimposed onto a parabolic trap potential, which holds a two-component Bose–Einstein condensate with (in general site-dependent) atom number N_i in each of its minima. Bottom: Each single condensate can be described by a pseudospin- $N_i/2$ degree of freedom at lattice site i , and neighbouring spins can be made to interact (dashed grey lines) by adjusting the optical lattice depth.

a spin- s to one of the spins of the chain through the unitary coupling operator $\exp(-i\lambda S_i \otimes \mathcal{S})$, where \mathcal{S} denotes the spin vector operator of the ancilla, S_i the spin vector operator at the i th lattice site of the chain, and λ is the coupling strength. The form of the coupling operator imposes selection rules and can facilitate only a restricted set of transitions between spin states, which are determined by the Clebsch–Gordan coefficients of the $S_i \otimes \mathcal{S}$ coupled basis. Coupling to a spin- s can change the spin- l by at most $2s$, which is a small relative change if $s \ll l$, which in turn poses restrictions on the effect of backaction. This intuition will be made precise in Sec. IV, where it is also shown that this constraint on the spin change implies a bound on the relative error of the temporal quantum correlation function measured by means of the ancilla-based measurement protocol.

Such an ancilla-based strong-measurement protocol is versatile and may be applied to a number of settings and experimental platforms. The application we had in mind, and which motivated the development of the measurement protocol, is an optical lattice holding an array of two-component Bose–Einstein condensates, each of which consists of some tens or hundreds of atoms. In the parameter regime speci-

fied in Ref. [10], each single condensate can be described by a one-axis twisting Hamiltonian $H_i = \chi(J_i^z)^2$ [11], where χ denotes the coupling strength and J_i^z is the z -component of a pseudospin- $N_i/2$ degree of freedom characterizing the N_i -atomic condensate at lattice site i . By adjusting the depth of the optical lattice, the pseudospins can be made to interact with each other; see Fig. 1 for an illustration. Following Refs. [12, 13], a beam of off-resonant light shone onto the i th condensate induces an interaction proportional to $S^z J_i^z$, where S^z denotes the z -component of the operator of the Stokes vector of the optical field integrated over the duration of the interaction. This operator representation of the Stokes vector is formally equivalent to a spin-1/2 operator, and hence the interaction $S^z J_i^z$ is equivalent to the coupling of a spin-1/2 to a spin- $N_i/2$, where the number N_i of atoms in the i th well is assumed to be much larger than 1.

II. SETTING

We consider a spatially extended system consisting of spin degrees of freedom on a lattice of arbitrary size, structure, and lattice dimension. To each lattice site i we assign a spin- l degree of freedom in the form of a local Hilbert space $\mathcal{H} = \mathbb{C}^{2l+1}$ for all i . The total system consisting of N spin- l degrees of freedom has therefore the system Hilbert space $\mathcal{H}_S = \mathcal{H}^{\otimes N}$. Time evolution of the spin system is generated by an arbitrary system Hamiltonian H acting on \mathcal{H}_S . (Generalization to nonunitary dynamics should be straightforward.)

Our goal is to extract two-time correlation functions of the type

$$C(t_1, t_2) = \langle O_1(t_1) O_2(t_2) \rangle, \quad (1)$$

where O_1 and O_2 are arbitrary observables on \mathcal{H}_S . We usually think of O_1 and O_2 as being supported on a single lattice site, or on a few adjacent lattice sites. Such a restriction is not necessary for the theoretical aspects of the protocol developed in the following, but it is expected to greatly facilitate an experimental implementation. $O_i(t_1) = e^{iHt_1} O_i e^{-iHt_1}$ denotes the observable O_i time-evolved in the Heisenberg picture under the Hamiltonian H until time t_1 .

III. MEASUREMENT PROTOCOL

For concreteness we aim at probing two-time correlations C of the z -components of spins at lattice sites i and j with respect to an arbitrary initial state $|\psi\rangle \in \mathcal{H}_S$,

$$C(t_1, t_2) = \langle S_i^z(t_1) S_j^z(t_2) \rangle = \langle \psi | e^{iHt_1} S_i^z e^{-iHt_1} e^{iHt_2} S_j^z e^{-iHt_2} | \psi \rangle, \quad (2)$$

where S_i^z denotes the z -component of the spin- l operator acting on lattice site i . The restriction to z -components is only for notational convenience; results for other components are obtained by using angular momentum eigenstates with respect to S^2 and some other spin component in the derivation reported below. Generalizations to correlations at more than

two times and/or more than two lattice sites should be feasible along similar lines.

We use a spin-1/2 degree of freedom as an ancilla, and hence $\mathcal{H}_A = \mathbb{C}^2$ and the total Hilbert space is

$$\mathcal{H}_{\text{tot}} = \mathcal{H}_S \otimes \mathcal{H}_A. \quad (3)$$

The system Hamiltonian $H = H_S \otimes \mathbb{1}_A$, which is responsible for the unitary evolution in the dynamic correlation function (2), acts nontrivially on \mathcal{H}_S only. In the following we outline a measurement protocol that allows us to determine a certain correlation function \mathcal{C} defined below. Subsequently, in Sec. IV, we show that the desired correlation function C can be extracted from \mathcal{C} under suitable conditions. The measurement protocol consists of the following steps.

a. Initial state preparation. We assume ancilla and system to initially be in a product state,

$$|\Psi\rangle = |\psi\rangle \otimes |\phi\rangle \equiv |\psi, \phi\rangle. \quad (4)$$

While the system initial state $|\psi\rangle$ is arbitrary (and determined by the physical situation under investigation), we choose

$$|\phi\rangle = \frac{1}{\sqrt{2}} (|-\rangle + |+\rangle) \quad (5)$$

for the ancilla initial state.

b. Time evolution until time t_1 . Time-evolve the initial state $|\Psi\rangle$ up to the time t_1 with the system Hamiltonian H_S ,

$$|\Psi(t_1)\rangle = e^{-iH_S t_1} |\psi\rangle \otimes |\phi\rangle \equiv |\psi(t_1), \phi\rangle. \quad (6)$$

The ancilla state $|\phi\rangle$ remains unaffected.

c. Coupling of the ancilla to system site i . Evolution of $|\Psi(t_1)\rangle$ with a unitary evolution operator

$$\mathcal{U}(\lambda) = \exp(-i\lambda S_i \otimes S), \quad (7)$$

which typically induces entanglement between the system and the ancilla. At the end of the coupling procedure one obtains

$$|\Psi_\lambda(t_1)\rangle = \mathcal{U}(\lambda) |\psi(t_1), \phi\rangle. \quad (8)$$

Attempts to use other coupling operators, in particular $\exp(-i\lambda S_i^x \otimes S^x)$ and $\exp(-i\lambda S_i^z \otimes S^z)$, have been unsuccessful so far; see Appendix A for details.

d. Measuring the ancilla. The ancilla is then probed by projectively measuring $\mathbb{1}_S \otimes S^z$, i.e., the z -component of the ancilla spin. We denote the two eigenstates of S^z as $|\pm\rangle$ with corresponding eigenvalues $\pm 1/2$. According to the Born rule, one measures the eigenvalues $+1/2$ and $-1/2$ with probabilities

$$P_\pm = \langle \Psi_\lambda(t_1) | (\mathbb{1}_S \otimes |\pm\rangle \langle \pm|) | \Psi_\lambda(t_1) \rangle. \quad (9)$$

The post-measurement state is given by the normalized projection onto the subspace corresponding to the outcome $\pm 1/2$ of the measurement,

$$|\Psi_\pm(t_1)\rangle = \frac{(\mathbb{1}_S \otimes |\pm\rangle \langle \pm|) |\Psi_\lambda(t_1)\rangle}{\|(\mathbb{1}_S \otimes |\pm\rangle \langle \pm|) |\Psi_\lambda(t_1)\rangle\|} \equiv |\psi_\pm(t_1)\rangle \otimes |\pm\rangle. \quad (10)$$

Ancilla and system are again in a product state.

e. Time evolution until time t_2 . Time-evolve the post-measurement state $|\Psi_{\pm}(t_1)\rangle$ up to the time t_2 with the system Hamiltonian H_S ,

$$|\Psi_{\pm}(t_2)\rangle = e^{-iH_S(t_2-t_1)} |\Psi_{\pm}(t_1)\rangle \otimes |\pm\rangle. \quad (11)$$

The ancilla state $|\pm\rangle$ remains unaffected.

f. Projective measurement at site j . At the final time t_2 , the disturbing effect due to a measurement is of no concern, and we can projectively measure the observable S_j^z at lattice site j without compromising the accuracy of the correlation function (2) that we wish to measure. We denote by $m \in \mathcal{S}$ the eigenvalues of S_j^z , where

$$\mathcal{S} = \{-l, -l+1, \dots, l-1, l\}. \quad (12)$$

The conditional probability of obtaining m when measuring S_j^z , after having obtained $\pm 1/2$ when measuring the ancilla, is

$$P_{m|\pm} = \langle \Psi_{\pm}(t_2) | (|m\rangle \langle m| \otimes \mathbb{1}_A) | \Psi_{\pm}(t_2) \rangle. \quad (13)$$

g. Correlating the measured outcomes. We use the probabilities (9) and (13) to calculate the correlation between the measured ancilla spin at t_1 and the system spin j at t_2 ,

$$\begin{aligned} \mathcal{C}(t_1, t_2) &= \sum_{m \in \mathcal{S}} m (P_{m|+} P_+ - P_{m|-} P_-) \\ &= \langle \Psi(t_1) | \mathcal{U}^\dagger(\lambda) (S_j^z(t_2 - t_1) \otimes S^z) \mathcal{U}(\lambda) | \Psi(t_1) \rangle, \end{aligned} \quad (14)$$

where the second line has been obtained by using the definitions introduced in this section and by making use of the spectral representations of S_j^z and of the ancilla spin S^z .

IV. RELATING \mathcal{C} TO C

In this section we show that the correlation function $\mathcal{C}(t_1, t_2)$ defined in Eq. (14) contains, under suitable conditions, terms proportional to the real, respectively imaginary, part of the desired two-time correlation function $C(t_1, t_2)$. A reader not interested in the details of the derivation may skip most of this section and continue reading from the main result (36). The assumptions made in the course of the derivation are summarized in Sec. VI.

The main tool for the calculation is to make use of the angular momentum-coupled basis when dealing with the spin-spin coupling operator $\mathcal{U}(\lambda)$ in Eq. (7), and to resort to the uncoupled basis when evaluating the effect of the ancilla spin operator S^z and when exploiting product properties of the initial state. The switching between the two bases is facilitated by means of Clebsch-Gordan coefficients.

We write the joint system-ancilla Hilbert space as a tensor product space consisting of three factors,

$$\mathcal{H}_{\text{tot}} = \mathcal{H}_i \otimes \mathcal{H}_A \otimes \mathcal{H}_{\text{rest}}, \quad (15)$$

where the Hilbert spaces \mathcal{H}_i and \mathcal{H}_A of lattice site i and the ancilla, respectively, are treated separately from the rest of the

system. We introduce a coupled basis $|l, j, m\rangle$ on the subspace $\mathcal{H}_i \otimes \mathcal{H}_A$, defined through the following eigenvalue equations,

$$S_i^2 |l, j, m\rangle = l(l+1) |l, j, m\rangle, \quad (16a)$$

$$S^2 |l, j, m\rangle = (3/4) |l, j, m\rangle, \quad (16b)$$

$$\mathbf{J}^2 |l, j, m\rangle = j(j+1) |l, j, m\rangle, \quad (16c)$$

$$J^z |l, j, m\rangle = m |l, j, m\rangle, \quad (16d)$$

where $\mathbf{J} = \mathbf{S}_i + \mathbf{S}$. We have $j \in \{l-1/2, l+1/2\}$ and $m \in \{-j, -j+1, \dots, j\}$ (and similarly for \tilde{j} and \tilde{m} introduced below). The coupled basis is particularly useful for evaluating the system-ancilla coupling unitary,

$$\begin{aligned} \mathcal{U}(\lambda) |l, j, m\rangle &= \exp[-i\lambda(\mathbf{J}^2 - S_i^2 - S^2)/2] |l, j, m\rangle \\ &= \exp\left[-i\lambda\left[j(j+1) - l(l+1) - \frac{3}{4}\right]/2\right] |l, j, m\rangle. \end{aligned} \quad (17)$$

To make use of this diagonal form of the coupling unitary, we expand the pre-coupling state at time t_1 in terms of the coupled basis,

$$|\Psi(t_1)\rangle = \sum_{j,m,\alpha} c_{jm} |l, j, m; \alpha\rangle, \quad (18)$$

where c_{jm} are complex-valued expansion coefficients and α denotes a set of quantum numbers labeling some basis of $\mathcal{H}_{\text{rest}}$. Inserting this expansion into the correlation function (14), we obtain

$$\begin{aligned} \mathcal{C} &= \sum_{j,m,\alpha} \sum_{\tilde{j},\tilde{m},\tilde{\alpha}} c_{j\tilde{m}}^* c_{jm\alpha} \varepsilon_{j\tilde{j}}(\lambda) \\ &\quad \times \langle l, \tilde{j}, \tilde{m}; \tilde{\alpha} | S_j^z(t_2 - t_1) \otimes S^z | l, j, m; \alpha \rangle \end{aligned} \quad (19)$$

with

$$\varepsilon_{j\tilde{j}}(\lambda) := \exp\left\{\frac{i\lambda}{2} [\tilde{j}(\tilde{j}+1) - j(j+1)]\right\}. \quad (20)$$

To shorten the notation, we will in the following omit the α quantum numbers and write

$$\mathcal{C} = \sum_{j,m} \sum_{\tilde{j},\tilde{m}} c_{j\tilde{m}}^* c_{jm} \varepsilon_{j\tilde{j}}(\lambda) \langle l, \tilde{j}, \tilde{m} | S_j^z(t_2 - t_1) \otimes S^z | l, j, m \rangle. \quad (21)$$

However, the reader should bear in mind that the derivation and the main result of this section hold for very general many-body systems, and not only for a single large spin coupled to a spin-1/2 ancilla.

The transformation to the uncoupled basis is, for the case of an arbitrary angular momentum l coupled to a spin-1/2, given by [14, Chap. 15.2]

$$|l, l \pm \frac{1}{2}, m\rangle = a_{lm} |l, m \mp \frac{1}{2}, \frac{1}{2}, \pm \frac{1}{2}\rangle \pm b_{lm} |l, m \pm \frac{1}{2}, \frac{1}{2}, \mp \frac{1}{2}\rangle \quad (22)$$

for all $|m| \leq l \pm 1/2$, with Clebsch-Gordan coefficients

$$a_{lm} = \sqrt{\frac{l+1/2+m}{2l+1}}, \quad b_{lm} = \sqrt{\frac{l+1/2-m}{2l+1}}. \quad (23)$$

Here, kets with four entries (compared to three entries for the coupled basis) denote the elements of the uncoupled basis, which satisfy the eigenvalue equations

$$S_i^2 |l, m_l, s, m_s\rangle = l(l+1) |l, m_l, s, m_s\rangle, \quad (24a)$$

$$S_i^z |l, m_l, s, m_s\rangle = m_l |l, m_l, s, m_s\rangle, \quad (24b)$$

$$S^2 |l, m_l, s, m_s\rangle = s(s+1) |l, m_l, s, m_s\rangle, \quad (24c)$$

$$S^z |l, m_l, s, m_s\rangle = m_s |l, m_l, s, m_s\rangle. \quad (24d)$$

Inserting (22) into (21) and using (24d) as well as the orthonormality of the basis states, we obtain

$$\begin{aligned} \mathcal{C} = \frac{1}{2} \sum_{m, \tilde{m}} & \left\{ \left\langle l, \tilde{m} - \frac{1}{2} \left| S_j^z(t_2 - t_1) \right| l, m - \frac{1}{2} \right\rangle \right. \\ & \times \left[c_{+, \tilde{m}}^* c_{+, m} a_{l\tilde{m}} a_{lm} + c_{-, \tilde{m}}^* c_{-, m} b_{l\tilde{m}} b_{lm} - c_{+, \tilde{m}}^* c_{-, m} a_{l\tilde{m}} b_{lm} e^{i\lambda(l+1/2)} - c_{-, \tilde{m}}^* c_{+, m} b_{l\tilde{m}} a_{lm} e^{-i\lambda(l+1/2)} \right] \\ & - \left\langle l, \tilde{m} + \frac{1}{2} \left| S_j^z(t_2 - t_1) \right| l, m + \frac{1}{2} \right\rangle \\ & \times \left[c_{+, \tilde{m}}^* c_{+, m} b_{l\tilde{m}} b_{lm} + c_{-, \tilde{m}}^* c_{-, m} a_{l\tilde{m}} a_{lm} + c_{+, \tilde{m}}^* c_{-, m} b_{l\tilde{m}} a_{lm} e^{i\lambda(l+1/2)} + c_{-, \tilde{m}}^* c_{+, m} a_{l\tilde{m}} b_{lm} e^{-i\lambda(l+1/2)} \right] \Big\}, \end{aligned} \quad (25)$$

where we have used the shorthand $c_{\pm, m} \equiv c_{l\pm 1/2, m}$. The ancilla-part of the expectation values has already been evaluated, and the remaining matrix elements in (25) involve only operators on and states from the system Hilbert space $\mathcal{H}_S = \mathcal{H}_i \otimes \mathcal{H}_{\text{rest}}$. (Recall that the α quantum numbers referring to $\mathcal{H}_{\text{rest}}$ have been omitted, and the matrix elements in (25) really involve many-body states and operators.)

The ancilla initial state, as well as the system state at time t_1 , are encoded in the expansion coefficients $c_{\pm, m}$, which, as is evident from (18), refer to the coupled basis. To make use of the properties of the ancilla initial state (5), we need to translate these coefficients into expansion coefficients with respect to the uncoupled basis. Making use of (18) and (22),

one obtains the identity

$$c_{\pm, m} = a_{lm} \gamma_m^\pm \pm b_{lm} \gamma_m^\mp, \quad (26)$$

where

$$\gamma_m^\pm = \langle l, m \mp \frac{1}{2}, \frac{1}{2}, \pm \frac{1}{2} | \Psi(t_1) \rangle \quad (27)$$

denote the expansion coefficients of $|\Psi(t_1)\rangle$ with respect to the uncoupled basis. The form of the ancilla initial state (5) implies that

$$\langle l, m, \frac{1}{2}, +\frac{1}{2} | \Psi(t_1) \rangle = \langle l, m, \frac{1}{2}, -\frac{1}{2} | \Psi(t_1) \rangle, \quad (28)$$

and hence $\gamma_{m+1}^+ = \gamma_m^-$. Inserting (26) into (25), and furthermore assuming $\gamma_{m+1}^\pm \approx \gamma_m^\pm \equiv \gamma_m$ (i.e., the expansion coefficients vary slowly with respect to m), we obtain

$$\begin{aligned} \mathcal{C} \approx \frac{1}{2} \sum_{m, \tilde{m}} & \gamma_m^* \gamma_m \left\{ \left\langle l, \tilde{m} - \frac{1}{2} \left| S_j^z(t_2 - t_1) \right| l, m - \frac{1}{2} \right\rangle \right. \\ & \times \left[(\tilde{a} + \tilde{b})(a + b) \tilde{a}a + (\tilde{a} - \tilde{b})(a - b) \tilde{b}b - (\tilde{a} + \tilde{b})(a - b) \tilde{a}b e^{i\lambda(l+1/2)} - (\tilde{a} - \tilde{b})(a + b) \tilde{b}a e^{-i\lambda(l+1/2)} \right] \\ & - \left\langle l, \tilde{m} + \frac{1}{2} \left| S_j^z(t_2 - t_1) \right| l, m + \frac{1}{2} \right\rangle \\ & \times \left[(\tilde{a} + \tilde{b})(a + b) \tilde{b}b + (\tilde{a} - \tilde{b})(a - b) \tilde{a}a + (\tilde{a} + \tilde{b})(a - b) \tilde{b}a e^{i\lambda(l+1/2)} + (\tilde{a} - \tilde{b})(a + b) \tilde{a}b e^{-i\lambda(l+1/2)} \right] \Big\}, \end{aligned} \quad (29)$$

where we used the shorthand notations $a \equiv a_{lm}$, $\tilde{a} \equiv a_{l\tilde{m}}$, $b \equiv b_{lm}$, and $\tilde{b} \equiv b_{l\tilde{m}}$. We further assume that the matrix

elements in (29) vary slowly with m , such that

$$\left\langle l, \tilde{m} \pm \frac{1}{2} \left| S_j^z(t_2 - t_1) \right| l, m \pm \frac{1}{2} \right\rangle \approx \left\langle l, \tilde{m} \left| S_j^z(t_2 - t_1) \right| l, m \right\rangle. \quad (30)$$

Under this condition, (29) simplifies to

$$\mathcal{C} \approx \sum_{m, \tilde{m}} \gamma_{\tilde{m}}^* \gamma_m \left\langle l, \tilde{m} \left| S_j^z(t_2 - t_1) \right| l, m \right\rangle (\tilde{a}b + a\tilde{b}) \\ \times \{ (a\tilde{a} - b\tilde{b})[1 - \cos(\lambda l)] + (\tilde{a}b - a\tilde{b})i \sin(\lambda l) \}, \quad (31)$$

where we have approximated $l + 1/2 \approx l$ in the trigonometric functions. Using the definitions of the Clebsch–Gordan coefficients (23) and approximating their denominators by $2l + 1 \approx 2l$, the correlation function can be rewritten as

$$\mathcal{C} \approx \frac{1}{2l} \sum_{m, \tilde{m}} \gamma_{\tilde{m}}^* \gamma_m \left\{ \left\langle l, \tilde{m} \left| \left[S_i^z, S_j^z(t_2 - t_1) \right] \right| l, m \right\rangle i \sin(\lambda l) \right. \\ \left. + 2 \left\langle l, \tilde{m} \left| S_i^z S_j^z(t_2 - t_1) \sqrt{1 - (S_i^z/S_i)^2} + \sqrt{1 - (S_i^z/S_i)^2} S_j^z(t_2 - t_1) S_i^z \right| l, m \right\rangle \sin^2(\lambda l/2) \right\} \\ = \frac{1}{2l} \left\langle \Psi(t_1) \left| \left(S_i^z, S_j^z(t_2 - t_1) \right) i \sin(\lambda l) + 2 \left(S_i^z S_j^z(t_2 - t_1) \sqrt{1 - (S_i^z/S_i)^2} + \sqrt{1 - (S_i^z/S_i)^2} S_j^z(t_2 - t_1) S_i^z \right) \sin^2(\lambda l/2) \right| \Psi(t_1) \right\rangle. \quad (32)$$

Assuming that we can approximate $\sqrt{1 - (S_i^z/S_i)^2} \approx 1$, the correlation function simplifies to

$$\mathcal{C} \approx \frac{1}{l} \left\langle \Psi(t_1) \left| \left\{ S_i^z, S_j^z(t_2 - t_1) \right\} \right| \Psi(t_1) \right\rangle \sin^2(\lambda l/2) \\ + \frac{i}{2l} \left\langle \Psi(t_1) \left| \left[S_i^z, S_j^z(t_2 - t_1) \right] \right| \Psi(t_1) \right\rangle \sin(\lambda l), \quad (34)$$

where the curly brackets denote the anticommutator. Using the definition of $|\Psi(t_1)\rangle$, this can be cast into the form

$$\mathcal{C} \approx \frac{2}{l} \text{Re} \left\langle \Psi \left| S_i^z(t_1) S_j^z(t_2) \right| \Psi \right\rangle \sin^2(\lambda l/2) \\ + \frac{1}{l} \text{Im} \left\langle \Psi \left| S_i^z(t_1) S_j^z(t_2) \right| \Psi \right\rangle \sin(\lambda l) \quad (35)$$

or, equivalently,

$$\mathcal{C} \approx \frac{2}{l} \sin^2(\lambda l/2) \text{Re} C(t_1, t_2) + \frac{1}{l} \sin(\lambda l) \text{Im} C(t_1, t_2), \quad (36)$$

which is the main result of this paper. Evidently, \mathcal{C} contains both, the real and imaginary parts of the desired two-time correlation function C defined in (2). A possible strategy for separating the real part from the imaginary part consists in measuring, according to the protocol of Sec. III, the correlation function \mathcal{C} at different coupling times/strength λ . For example, choosing $\lambda l = \pi$ gives

$$\mathcal{C}(\lambda l = \pi) \approx \frac{2}{l} \text{Re} C(t_1, t_2), \quad (37)$$

from which an estimate of $\text{Re} C$ can be obtained. By further measuring an estimate of \mathcal{C} at $\lambda l = \pi/2$,

$$\mathcal{C}(\lambda l = \pi/2) \approx \frac{1}{l} \text{Re} C(t_1, t_2) + \frac{1}{l} \text{Im} C(t_1, t_2), \quad (38)$$

$$\mathcal{C} \approx \frac{1}{2l} \sum_{m, \tilde{m}} \gamma_{\tilde{m}}^* \gamma_m \left\langle l, \tilde{m} \left| S_j^z(t_2 - t_1) \right| l, m \right\rangle \left\{ (\tilde{m} - m)i \sin(\lambda l) \right. \\ \left. + 2 \left(\tilde{m} \sqrt{1 - (m/l)^2} + m \sqrt{1 - (\tilde{m}/l)^2} \right) \sin^2(\lambda l/2) \right\}. \quad (32)$$

Making use of the spectral theorem, we write

and making use of the knowledge of $\text{Re} C$, the imaginary part $\text{Im} C$ can be extracted. More generally, Fourier analysis can be used to extract real and imaginary parts of C from estimators of \mathcal{C} at multiple and arbitrarily spaced values of λl .

V. EXAMPLE: TWO SPIN- l COUPLED TO SPIN-1/2

We illustrate the performance of the protocol of Sec. III, and also its statistical and systematic errors, by studying a simple system consisting of two coupled spin- l degrees of freedom, augmented by a spin-1/2 ancilla used for probing at the early time t_1 . The total Hilbert space is

$$\mathcal{H}_{\text{tot}} = \mathcal{H}_1 \otimes \mathcal{H}_2 \otimes \mathcal{H}_A \quad (39)$$

with $\mathcal{H}_1 = \mathbb{C}^{2l+1} = \mathcal{H}_2$ and $\mathcal{H}_A = \mathbb{C}^2$. For the system Hamiltonian we choose a Heisenberg coupling between the two spin- l degrees of freedom,

$$H_S = S_1 \otimes S_2 \otimes \mathbb{1}_A. \quad (40)$$

Our goal is to measure the normalized two-time correlation function

$$C(t_1, t_2) = \frac{\langle S_1^z(t_1) S_2^z(t_2) \rangle}{l^2} \quad (41)$$

with respect to initial states specified further below. The ancilla initial state and the system–ancilla coupling are as specified in Eqs. (5) and (7). To obtain the correlation function \mathcal{C} in Eq. (14), we need to calculate the probabilities (9) and (13), which are given as expectation values of certain projection operators. For the 3-spin example considered here, these expectation values can be numerically computed in Mathematica for moderate spin quantum numbers l .

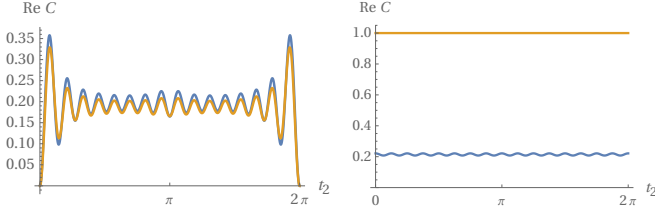


FIG. 2. Real parts of two-time correlation functions $C(t_1, t_2)$ as defined in (41) for spin quantum number $l = 8$, plotted for $t_1 = 0$ as a function of t_2 . Orange lines show exact correlation functions, blue lines are estimates based on Eqs. (37) and (14). Left: Starting from the uniform initial state (42), which satisfies the condition of slowly varying expansion coefficients γ_m^\pm , good agreement between exact and estimated correlations is observed. Right: For the maximally magnetized initial state (43), the coefficients γ_m^\pm are not slowly varying in m , hence the conditions for the validity of the measurement protocol are not satisfied, leading to a large discrepancy between exact and estimated correlations.

For this setting, we show in Fig. 2 the real part of the exact correlation function (41), and compare it to the estimate calculated via (37) and (14). The left plot in Fig. 2 is for a system initial state

$$\frac{1}{2l+1} \sum_{m_1, m_2=-l}^l |l, m_1\rangle \otimes |l, m_2\rangle, \quad (42)$$

in which all S_i^z eigenstates are equally populated, and as a result the expansion coefficients γ_m^\pm vary slowly with m , as required for the measurement protocol. Indeed, Fig. 2 (left) shows good agreement between the exact two-time correlation function and its measured approximation. In contrast, the system initial state

$$|l, l\rangle \otimes |l, l\rangle, \quad (43)$$

which has rapidly varying expansion coefficients γ_m^\pm , leads to a substantial discrepancy between the exact correlations and their measured counterpart (Fig. 2, right).

In addition to slowly varying γ_m^\pm , the protocol of Sec. III also requires a large spin quantum number l , and estimators of the two-time correlation function C are expected to be more accurate the larger l is. To explore how the accuracy of the measured estimator depends on the spin quantum number l , we use as a system initial state a normalized version of

$$\sum_{m_1=-l}^l (l - m_1) |l, m_1\rangle \otimes |l, l\rangle \quad (44)$$

and calculate correlations for various spin quantum numbers l . For this choice, the measured estimator deviates significantly from the exact correlation function for $l = 4$ (Fig. 3 left), but the agreement improves rapidly when increasing the spin quantum number to $l = 16$ (Fig. 3 right).

The plots in Figs. 2 and 3 are based on Eqs. (37) and (14), making use of the probabilities $P_\pm P_{m|\pm}$ calculated according to Eqs. (9) and (13). In an experimental realization of the

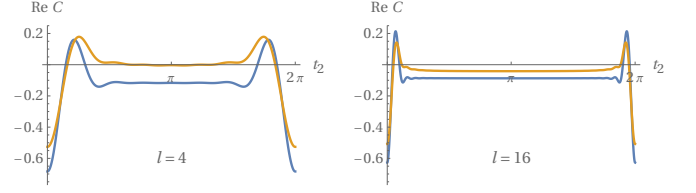


FIG. 3. Real parts of two-time correlation functions $C(t_1, t_2)$ as defined in (41) starting from the initial state (44), plotted for $t_1 = 0$ as a function of t_2 . Orange lines show the exact correlation functions, blue lines are estimates based on Eqs. (37) and (14), which correspond to the outcome of the measurement protocol of Sec. III in the limit of a large number of measurement runs. Hence, in the absence of statistical errors from finite sample sizes, the differences between the orange and the blue lines illustrate the systematic error stemming from large- l expansions and approximations in the derivation of the measurement protocol. For $l = 4$ (left panel) the systematic error is significant, but shrinks rapidly with increasing spin quantum numbers $l = 16$ (right panel).

measurement protocol of Sec. III, however, the exact probability distributions are not available, but have to be estimated as a sample average over repeated runs of the protocol. To obtain the exact probabilities $P_\pm P_{m|\pm}$ in principle requires an infinite sample of runs and is not realistic. Finite samples, on the other hand, introduce errors in P_\pm and $P_{m|\pm}$, which by error propagation result in statistical errors in the correlation function C , on top of the systematic errors discussed above and illustrated in Figs. 2 and 3. To assess the magnitude of these statistical errors we proceed as follows: From the probability distribution $P_\pm P_{m|\pm}$ we draw samples of size \mathcal{N}_s . Each element of the sample represents the outcome $(\pm 1/2, m)$ of a hypothetical measurement according to the protocol of Sec. III. To mimic experimental constraints we use, instead of the exact probabilities $P_\pm P_{m|\pm}$, the relative frequencies of the outcomes $(\pm 1/2, m)$ within a random sample. The larger the sample size, the smaller is the statistical error in the probabilities, and hence also in the correlation function C . To estimate the size of these statistical errors for a given sample size \mathcal{N}_s , we calculate C not only from one sample, but for 100 samples of size \mathcal{N}_s . Each of those samples will give a slightly different value of C , and we calculate the standard deviation of these fluctuating values, which serves as an estimate of the statistical error in C .

Figure 4 shows, for the uniform initial state (42), the t_2 -dependence of the two-time correlation function $C(0, t_2)$ estimated according to our measurement protocol, together with the (likewise t_2 -dependent) statistical errorbars obtained according to the procedure described in the previous paragraph. For sample size $\mathcal{N}_s = 100$ the statistical errors are considerable (Fig. 4 left), but already for $\mathcal{N}_s = 1000$ statistical fluctuations are smaller than the systematic errors that result from the approximations in the measurement protocol of Sec. III (Fig. 4 right). A rough estimate based on the available data suggests that statistical error bars of C scale like $\mathcal{N}_s^{-1/2}$ with the sample size. Moreover we find, for fixed sample size \mathcal{N}_s and at least for spin quantum numbers l up to 32 for which we have data, that statistical errors are essentially independent of l (not shown in the plots).

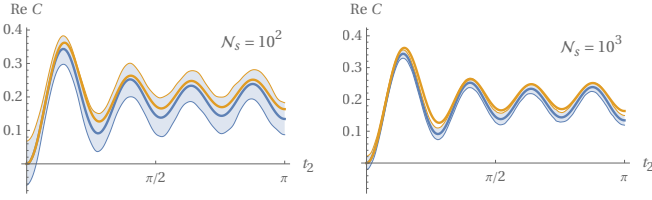


FIG. 4. Illustration of the magnitude of statistical fluctuations in the two-time correlations C for $l = 4$, obtained according to the protocol of Sec. III from measurement samples of finite size. Real parts of the exact two-time correlation functions $C(0, t_2)$, starting from the uniform initial state (42), are plotted as orange lines. Blue lines show estimates of C obtained according to Eqs. (37) and (14) with the exact probabilities $P_{\pm}P_{m|\pm}$, which corresponds to using measurement samples of infinite size. The blue shaded areas around the blue lines indicate statistical error bars of one standard deviation, calculated according to the procedure described in the text for measurement samples of finite size. For sample size $N_s = 100$ (left panel) statistical fluctuations are the dominant source of errors, larger than the systematic deviation between the estimated (blue) and exact (orange) values. For sample size $N_s = 1000$ (right panel) statistical fluctuations are significantly reduced and are smaller than systematic errors.

VI. SUMMARY AND CONCLUSIONS

To experimentally determine two-time quantum correlation according to the protocol proposed in this paper, the key task is to determine sufficiently accurate estimators of the probabilities $P_{\pm}P_{m|\pm}$ defined in Eqs. (9) and (13). These probabilities describe the likelihood of measuring $\pm 1/2$ for the ancilla spin component S^z , followed by a measurement result m for the component S_j^z of the spin at site j . Estimators of the probabilities $P_{\pm}P_{m|\pm}$ can therefore be obtained as the relative frequencies of the outcome pairs (\pm, m) recorded over a sufficiently large sample of measurements. Each run follows the measurement protocol of Sec. III, which consists of the following steps:

- (a) Prepare the spin-1/2 ancilla in the state (5).
- (b) Time-evolve the system until time t_1 .
- (c) Couple system and ancilla by means of the unitary (7).
- (d) Measure the ancilla observable S^z .
- (e) Time-evolve the system until time t_2 .
- (f) Measure the system observable S_j^z .

Recording the measurement outcomes and repeating the above steps multiple times, estimators of the probabilities (9) and (13) are obtained. From these probabilities the correlation function \mathcal{C} as defined in (14) can be computed. Repeating the above steps (a)–(f) for several couplings λ then gives access to the real and imaginary parts of \mathcal{C} separately, as discussed at the end of Sec. IV.

The measured correlation function (14) is, under suitable assumptions, related to the desired correlation function C via Eq. (36). The assumptions that went into the calculation of this relation are:

- (i) Large spin quantum number $l \gg 1$ of the spin at lattice site i . This is only really needed when going from (33) to (34) by assuming $\sqrt{1 - (S_i^z/S_i)^2} \approx 1$. This is a shorthand notation for the actual requirement that only those expectation values in the expansion (32) contribute significantly to \mathcal{C} for which $(\tilde{m}/l)^2 \ll 1$ and $(m/l)^2 \ll 1$. At other instances in the derivation, $l \gg 1$ is only assumed for the convenience of shorter expressions; replacing occurrences of l by $l + 1/2$ in (36) will undo these further approximations.
- (ii) The expansion coefficients γ_m^{\pm} (27) of the system state at t_1 vary slowly with m , such that $\gamma_{m+1}^{\pm} \approx \gamma_m^{\pm}$.
- (iii) Assumption (30) on the matrix elements of $S_j^z(t_2 - t_1)$ is condition (ii) in disguise: the matrix elements are required to be slowly varying in m .

While the largeness of the spin quantum number l in condition (i) should be easy to assess, the slowly varying expansion coefficients γ_m^{\pm} required in assumptions (ii) and (iii) may require additional experimental effort. In principle the coefficients γ_m^{\pm} may be obtained in a separate series of experimental runs in which the spin component S_i^z at site i is measured at time t_1 and relative frequencies of the outcomes are recorded.

An experimental platform in which an assembly of interacting large spins can be realized, and in which the protocol proposed in this paper can potentially be implemented, is discussed in Sec. I and sketched in Fig. 1. Other suitable platforms, based for example on multiply-degenerate ground-state manifolds, are expected to be feasible as well. Potential physical application of the thus obtained two-time correlation functions include the analysis of temporal universality in the vicinity of quantum phase transitions, or of signatures of slow relaxation in quantum glasses. Since both these mentioned applications are genuine many-body phenomena, we conclude by re-emphasizing that, even though Sec. V treats a simple two-spin system for illustrative purposes, the protocol put forward in this paper is suited for proper many-body applications and can in principle be applied to large- l spin systems of arbitrary lattice dimension and lattice size.

ACKNOWLEDGMENTS

Discussions with Markus Oberthaler, which initiated the study reported in this paper, are gratefully acknowledged.

Appendix A: System–ancilla coupling $S_i^z \otimes S^z$

The measurement protocol of Sec. III makes use of a system–ancilla coupling of Heisenberg type (7). In this appendix we consider an alternative, namely a coupling unitary $\mathcal{U}(\lambda) = \exp(-i\lambda S_i^z \otimes S^z)$ of Ising type. Since the uncoupled basis states $|l, m_l, s, m_s\rangle$ are eigenstates of the system spin operator S_i^z as well as of the ancilla spin operator S^z , no need for

the use of a coupled basis arises. Expanding

$$|\Psi(t_1)\rangle = \sum_{m_l, m_s} c_{m_l m_s} |l, m_l, s, m_s\rangle \quad (\text{A1})$$

in the uncoupled basis, we can write (14) as

$$\begin{aligned} \mathcal{C} &= \sum_{m_l, m_s} \sum_{\tilde{m}_l, \tilde{m}_s} c_{\tilde{m}_l \tilde{m}_s}^* c_{m_l m_s} \exp[i\lambda(\tilde{m}_l \tilde{m}_s - m_l m_s)] \\ &\quad \times \langle l, \tilde{m}_l, s, \tilde{m}_s | S_j^z(t_2 - t_1) \otimes S^z | l, m_l, s, m_s \rangle \\ &= \frac{1}{2} \sum_{m_l, \tilde{m}_l} \left(c_{\tilde{m}_l +}^* c_{m_l +} e^{i\lambda(\tilde{m}_l - m_l)} \langle l, \tilde{m}_l | S_j^z(t_2 - t_1) | l, m_l \rangle \right. \\ &\quad \left. - c_{\tilde{m}_l -}^* c_{m_l -} e^{-i\lambda(\tilde{m}_l - m_l)} \langle l, \tilde{m}_l | S_j^z(t_2 - t_1) | l, m_l \rangle \right). \end{aligned} \quad (\text{A2})$$

The form of the ancilla initial state (5) implies $c_{m_l +} = c_{m_l -} \equiv c_{m_l}$ for all m_l , which allows us to write

$$\mathcal{C} = \sum_{m_l, \tilde{m}_l} c_{\tilde{m}_l}^* c_{m_l} \sin[\lambda(\tilde{m}_l - m_l)] \langle l, \tilde{m}_l | S_j^z(t_2 - t_1) | l, m_l \rangle \quad (\text{A3})$$

or, by making use of the spectral theorem,

$$\begin{aligned} \mathcal{C} &= \frac{1}{2} \left\langle \Psi(t_1) \left| e^{i\lambda S_i^z} S_j^z(t_2 - t_1) e^{-i\lambda S_i^z} \right| \Psi(t_1) \right\rangle \\ &\quad - \frac{1}{2} \left\langle \Psi(t_1) \left| e^{-i\lambda S_i^z} S_j^z(t_2 - t_1) e^{i\lambda S_i^z} \right| \Psi(t_1) \right\rangle. \end{aligned} \quad (\text{A4})$$

Unfortunately, it is not evident how the two-time correlation function (2) can be extracted from this quantity, except in the limit of small λ , which amounts to recovering one of the results of Ref. [7].

The coupling unitary $\mathcal{U}(\lambda) = \exp(-i\lambda S_i^x \otimes S^x)$ leads to similar results, only with $\sin[\lambda(\tilde{m}_l - m_l)]$ replaced by $\cos[\lambda(\tilde{m}_l + m_l)]$ in Eq. (A3).

-
- [1] R. Kubo, “Statistical-mechanical theory of irreversible processes. I. General theory and simple applications to magnetic and conduction problems,” *J. Phys. Soc. Jpn.* **12**, 570–586 (1957).
 - [2] R. J. Glauber, “The quantum theory of optical coherence,” *Phys. Rev.* **130**, 2529–2539 (1963).
 - [3] R. Zwanzig, “Time-correlation functions and transport coefficients in statistical mechanics,” *Annu. Rev. Phys. Chem.* **16**, 67–102 (1965).
 - [4] B. Sciolia, D. Poletti, and C. Kollath, “Two-time correlations probing the dynamics of dissipative many-body quantum systems: Aging and fast relaxation,” *Phys. Rev. Lett.* **114**, 170401 (2015).
 - [5] O. Romero-Isart, M. Rizzi, C. A. Muschik, E. S. Polzik, M. Lewenstein, and A. Sanpera, “Quantum memory assisted probing of dynamical spin correlations,” *Phys. Rev. Lett.* **108**, 065302 (2012).
 - [6] M. Knap, A. Kantian, T. Giamarchi, I. Bloch, M. D. Lukin, and E. Demler, “Probing real-space and time-resolved correlation functions with many-body Ramsey interferometry,” *Phys. Rev. Lett.* **111**, 147205 (2013).
 - [7] P. Uhrich, S. Castrignano, H. Uys, and M. Kastner, “Noninvasive measurement of dynamic correlation functions,” *Phys. Rev. A* **96**, 022127 (2017).
 - [8] M. Kastner and P. Uhrich, “Reducing backaction when measuring temporal correlations in quantum systems,” *Eur. Phys. J. Spec. Top.* **227**, 365–378 (2018).
 - [9] P. Uhrich, C. Gross, and M. Kastner, “Probing unitary two-time correlations in a neutral atom quantum simulator,” *Quantum Sci. Technol.* **4**, 024005 (2019).
 - [10] W. Muessel, H. Strobel, D. Linnemann, D. B. Hume, and M. K. Oberthaler, “Scalable spin squeezing for quantum-enhanced magnetometry with Bose–Einstein condensates,” *Phys. Rev. Lett.* **113**, 103004 (2014).
 - [11] M. Kitagawa and M. Ueda, “Squeezed spin states,” *Phys. Rev. A* **47**, 5138–5143 (1993).
 - [12] A. Kuzmich, N. P. Bigelow, and L. Mandel, “Atomic quantum non-demolition measurements and squeezing,” *Europhys. Lett.* **42**, 481–486 (1998).
 - [13] A. Kuzmich and E. S. Polzik, “Atomic quantum state teleportation and swapping,” *Phys. Rev. Lett.* **85**, 5639–5642 (2000).
 - [14] R. Shankar, *Principles of Quantum Mechanics*, 2nd ed. (Springer, New York, 1994).